Distribution Agreement

In presenting this thesis as a partial fulfillment of the requirements for a degree from Emory University, I hereby grant to Emory University and its agents the non-exclusive license to archive, make accessible, and display my thesis in whole or in part in all forms of media, now or hereafter now, including display on the World Wide Web. I understand that I may select some access restrictions as part of the online submission of this thesis. I retain all ownership rights to the copyright of the thesis. I also retain the right to use in future works (such as articles or books) all or part of this thesis.

Jacob Fontaine April 12, 2022

Culture-Based Methods Provide Critical Phenotypic Ecological Characteristics of Bacteria and their Bacteriophage Undiscernible via Genomics

by

Jacob Fontaine

Bruce Levin
Adviser

Department of Biology

Bruce Levin

Adviser

Michael Woodworth

Committee Member

Nic Vega

Committee Member

2022

Culture-Based Methods Provide Critical Phenotypic Ecological Characteristics of Bacteria and their Bacteriophage Undiscernible via Genomics

By

Jacob Fontaine

Bruce Levin

Adviser

An abstract of
a thesis submitted to the Faculty of Emory College of Arts and Sciences
of Emory University in partial fulfillment
of the requirements of the degree of
Bachelor of Science with Honors

Department of Biology

2022

Abstract

Culture-Based Methods Provide Critical Phenotypic Ecological Characteristics of Bacteria and their Bacteriophage Undiscernible via Genomics

By Jacob Fontaine

Despite a massive amount of research, the population dynamic, ecological, and evolutionary mechanisms that determine the distribution and abundance of microbes in the human gut microbiome have yet to be determined. Using fecal microbiota transplantation (FMT) doses as a proxy for the human gut microbiome, we have employed molecular and culture-based methods to investigate such mechanisms for *Escherichia coli* in the gut. Genetic analysis suggests there is little genetic variation among isolates of *E. coli* and among the their lytic phages. Nevertheless, there is phenotypic variation. While all *E. coli* isolates tested are susceptible to the FMT-sourced phages, there is substantial quantitative variation across the bacteria in their susceptibility to the phage and in the capacity of the phage to infect the different isolates of the bacteria. Taken at large, the results of this study question whether the purely correlative and bioinformatic analysis conventionally used to study microbiomes is able to elucidate the mechanisms that determine the structure of these microbial communities.

Culture-Based Methods Provide Critical Phenotypic Ecological Characteristics of Bacteria and their Bacteriophage Undiscernible via Genomics

By

Jacob Fontaine

Bruce Levin, PhD

Adviser

A thesis submitted to the Faculty of Emory College of Arts and Sciences
of Emory University in partial fulfillment
of the requirements of the degree of
Bachelor of Science with Honors

Department of Biology

2022

Acknowledgements

We would like to acknowledge Candace Miller for research support and coordination of sample delivery and the Emory University Hospital Clinical Microbiology laboratory for use of their VITEK2 bacterial susceptibility and identification platform. We would also like to acknowledge Dr. Rodrigo García and Brandon Berryhill for intellectual advisement on this project, and David Goldberg for extraction of bacterial and phage genomic DNA and sequencing.

Table of Contents

Introduction

Each human possesses trillions of microorganism in their GI tract with which they have a symbiotic, or potentially pathologic, relationship. The gut microbiome is a burgeoning field of study and part of a larger shift that incorporate resident microorganisms in a better understanding of human health and disease. Unhealthy gut microbiome compositions, often described as dysbiosis, has been linked to weight gain and obesity, characterizes enteric disorders such as inflammatory bowel disease (IBD) and irritable bowel syndrome (IBS), and has even been postulated as a contributing factor of neurodegenerative disorders (Amabebe et. al., 2021; Wang et. al., 2020; Canakis et. al., 2020; Ni et. al., 2017; Sarkar et. al., 2019; Chidambaram et. al., 2022). One of the best established causes of gut dysbiosis is antibiotic exposure (McDonnell et. al., 2021; Schwartz et. al., 2020; Zhang et. al., 2021). The antibiotic-induced dysbiotic state is concurrent with enteric infection, which can increase risk for *Clostridioides difficile* infection (CDI) (Leffler and Lamont, 2015; Smits et. al., 2016; Theriot and Young, 2015). CDI is the most common nosocomial infection, with just under half a million cases each year resulting in approximately 29,000 deaths (Lessa et. al., 2015; Samore et. al., 1999). *C. difficile* is inherently resistant to most antibiotic classes, but resistance to first line treatments for CDI is also increasing. Recurrence is a characteristic feature of CDI, and anywhere from 20%-30% of patients suffer from rCDI even after antibiotic treatment (Doh et. al., 2014; Madoff et. al., 2020; Pepin et. al., 2005; Sheitoyan-Pesant et. al., 2016; Spigaglia et. al., 2018)

A promising approach to the treatment of such infections are fecal microbiota transplants (FMTs). This treatment consists of healthy donor stool being directly transferred into the gut of an ill recipient, typically delivered via colonoscopy, swallowed capsules, gastric feeding tube, or enema. Several diseases and disorders have been experimentally treated with FMTs, FMTs are best understood in the context of treatment for rCDI. FMTs are classified as an investigational new drug by the United States Food and Drug Administration (FDA), which has elected to exercise enforcement discretion in the use of FMT for cases of rCDI that are not responsive to conventional therapies. Despite their lack of standardization as treatment, reviews of FMTs boast a ~90% clearance rate of rCDI with only 1 or 2 treatments (Gough et. al., 2011; Lai et. al., 2019; Ooijevaar et. al., 2018). FMTs also consistently have a higher success rate at clearing rCDI than vancomycin, one of the most commonly used antibiotics to treat CDI and rCDI (Cammarota et. al., 2015; Hota et. al., 2017; van Nood et. al., 2013).

The potential mechanisms by which FMT may effectively treat rCDI and other disorders are not well understood. Restoration of the healthy state of the gut microbiome is characteristic of recovery, but how the healthy state is achieved remains unclear (Fujimoto et. al., 2021; Khoruts et. al., 2016; Sokol et. al., 2020; Weingarden et. al., 2014). Elucidating the forces driving the strain and species composition of the gut microbiome is critical for understanding gut ecology and for advancing the precision of microbiome therapies to move beyond the use of FMT. Paramount to these investigations is the consideration of the gut microbiome as a microbial community, and not simply as a collection of bacteria. Bacteriophage (phage) are universally present in the gut microbiome, yet the gut virome hasn't been as extensively investigated as the bacterial fraction of the gut microbiome (Mirzaei et. al., 2017). There is evidence supporting that phage exert significant selective pressure on gut bacteria and play a crucial role in FMT treatment of CDI (Ott et. al., 2017). Bacteria-free FMT filtrate was administered to 5 patients with rCDI, all of whom recovered with no symptoms after 4 days, which remained over 2 years. Ott et. al. found that both the bacteriome and the virome of the patients changed after treatment to match that of the donor.

Because many taxa that reside in the gut are strict anaerobes that are challenging to culture, research investigating the gut microbiome largely depends on bioinformatic approaches. Metagenomics is a powerful tool used to assess and track the higher-order taxonomic diversity of the bacteriome, virome, and mycobiome of the human gut, as well as investigate prevalence of genes of interest. However, while phage can be characterized into taxonomic families by genomic nucleic acid sequences, phenotype inference from sequence data has lagged for phage. Phage host range and infectivity are important ecological properties that cannot presently be fully determined using sequence data alone. Assessing the ecological role of phage in the gut microbiome, and in FMTs, requires integrated analysis of culture-based and genomic bioinformatic methods. We show that combining these techniques yields novel insights beyond either approach alone.

We present an assessment of diversity of gut *Escherichia coli* and their phages within the context of FMTs. A bank was created of *E. coli* isolates and *E. coli* phage isolates sourced from clinical FMT doses produced by Emory Microbiome Enrichment Program. FMT doses manufactured modifying the methods previously described, by increasing the stool content to 40% w/v (Tauxe et. al., 2016). Bacterial and phage Isolates underwent whole-genome sequencing to assess genetic variation. To evaluate the phenotypic variation, an infection network was created showing host range and infectivity of phage isolates.

We show here that genomic analyses alone would not have predicted the extend of observed phenotypic diversity in bacteria and phage isolates from an individual over a one month period. Bioinformatic analysis showed high genetic homology among 8 FMT-sourced *E. coli* isolates, with few variable genes and few SNPs among common genes. Construction of an infection network showing efficiency of plating of each *E. coli* and phage isolate revealed that individual phages had significant difference of plaquing efficiency on genetically similar *E. coli*, and conversely that individual bacteria showed significant differences of sensitivity to genetically similar phages.

Results

Initial density of aerobic bacteria in FMT doses ranges from 10^5-10^7 CFU/mL (data not shown). 16S sequencing of 10 randomly chosen colonies cultured from plates of each of 3 FMT doses from 2 donors show that a majority of the fast-growing aerobically cultured bacteria are *E. coli* or a closely related bacteria (Fig. 1A, Table S1). 8 randomly chosen isolates from a single patient comprised a bank of *E. coli* to serve as a pseudo-representative sample of *E. coli* from the donor's FMTs: A1, A3, A4, A9, B6, B9, C2L, and D4L. Bank isolates show high genetic similarity, each possessing the same *in silico* MLST profile, 4774, as well as pan-susceptibility to 18 clinically-relevant antibiotics (Ampicillin/Sulbactam, Piperacillin/Tazobactam, Cefazolin, Cefoxitin, Ceftazidime, Ceftriaxone, Cefepime, Ertapenem, Meropenem, Amikacin, Gentamicin, Tobramycin, Levofloxacin, Tetracycline, Tigecycline, Nitrofurantoin, Trimethoprim/Sulfamethoxazole). These isolates were also highly similar by genomic analysis; isolates differed by an average of only 32 ± 17 single nucleotide polymorphisms (SNPs) among core genes (Fig. 1B). Isolates' also possessed as single plasmid which showed homology in RFLP analysis. Isolate plasmids were extracted and digested with 4 restriction endonucleases, and isolate plasmids showed no variation in fragment lengths via gel electrophoresis (Fig. 1C). Across bank isolates' whole genomes, among 4364 aligned gene clusters, there were only 37 variably detected genes. Isolates with the most SNPs and the fewest SNPs were grouped into 2 putative Clades based on published threshold of 17 SNPs used for

outbreak investigation for additional comparisons. Comparing isolates in these two putative Clades using pangenomic analyses with prokka and roary identified 8 genes that were differentially present/absent (Table 1). Clade 1 members had 6 genes that were not detected in Clade 2, several of which are transposases. This Clade also had a low SNP count, with an average of 9 ± 3 SNPs. Clade two had 2 genes not detected in Clade 1, and a SNP average of 34 ± 23 SNPs.

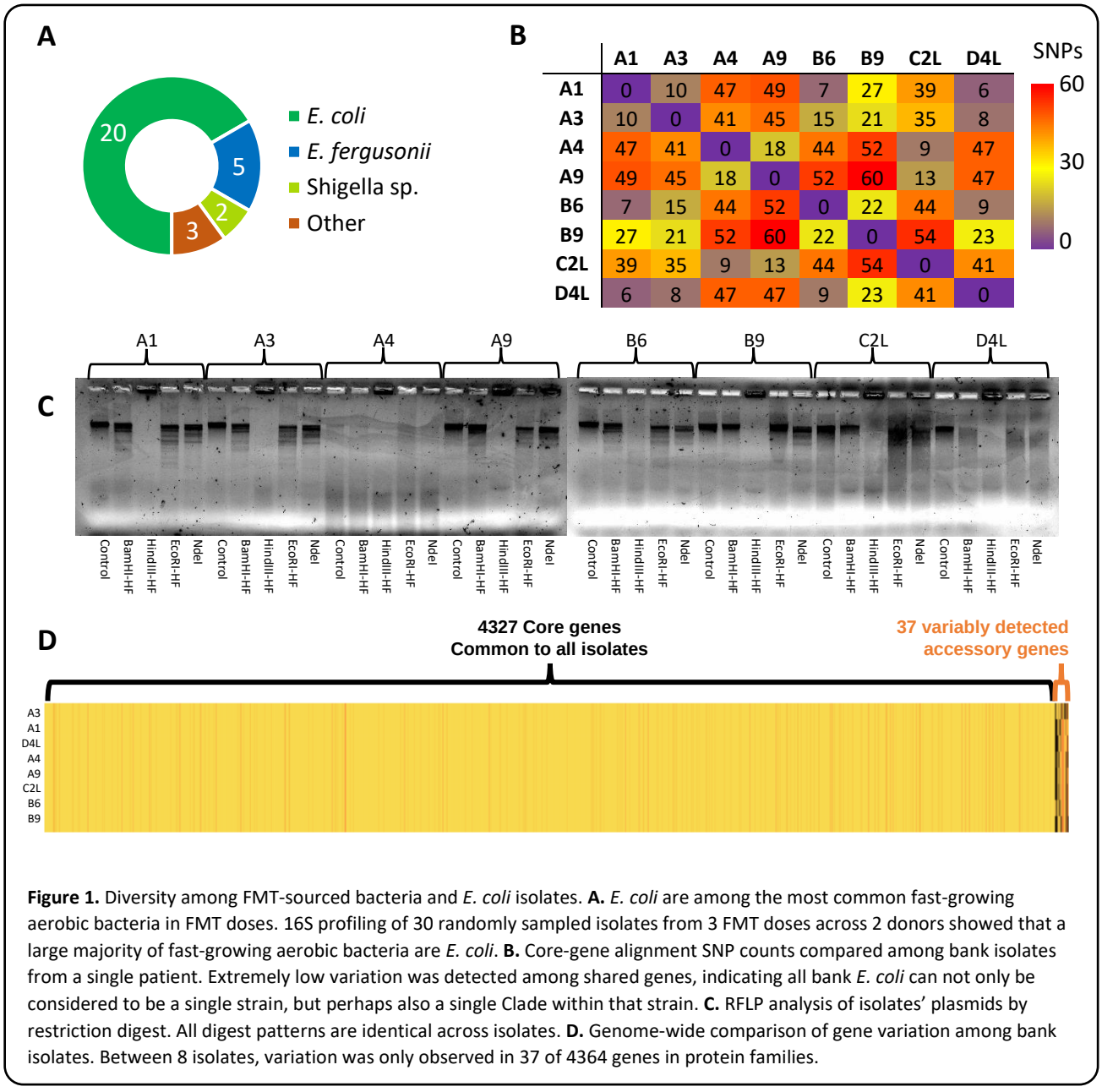

	A1	A3	A4	A9	B6	B9	C2L	D4L
A1	0	10	47	49	7	27	39	6
A3	10	0	41	45	15	21	35	8
A4	47	41	0	18	44	52	9	47
A9	49	45	18	0	52	60	13	47
B6	7	15	44	52	0	22	44	9
B9	27	21	52	60	22	0	54	23
C2L	39	35	9	13	44	54	0	41
D4L	6	8	47	47	9	23	41	0

Figure 1. Diversity among FMT-sourced bacteria and *E. coli* isolates. **A.** *E. coli* are among the most common fast-growing aerobic bacteria in FMT doses. 16S profiling of 30 randomly sampled isolates from 3 FMT doses across 2 donors showed that a large majority of fast-growing aerobic bacteria are *E. coli*. **B.** Core-gene alignment SNP counts compared among bank isolates from a single patient. Extremely low variation was detected among shared genes, indicating all bank *E. coli* can not only be considered to be a single strain, but perhaps also a single Clade within that strain. **C.** RFLP analysis of isolates' plasmids by restriction digest. All digest patterns are identical across isolates. **D.** Genome-wide comparison of gene variation among bank isolates. Between 8 isolates, variation was only observed in 37 of 4364 genes in protein families.

For further comparisons for breadth of infectivity of the isolated phages, two additional *E. coli* isolates, G1 and G3, were cultured from a 2nd FMT donor, as well as a laboratory strain of *E. coli* C also underwent whole genome sequencing and *in silico* MLST profiling. One of these isolates, G3, was found to have the same MLST profile as the bank isolates, 4774, while the other, G1, and *E. coli* C had distinct

MLST profiles, 1721 and 73 respectively. While each individual may have strains more unique to their gut microbiome, there may be some commonality among *E. coli* in the gut, though this investigation at the strain level requires further investigation and is beyond the scope of this paper.

Table 1. Clade formation among bank *E. coli*. Many annotations of variably detected gene clusters are transposases. Average SNP counts were lower for Clade 1 isolates compared to Clade 2 isolates.

Gene Cluster	Clade One (A1, A3, B6, D4L)	Clade Two (A4, A9, B9, C2L)
IS1 family transposase	X	
IS3 family transposase ISSen4	X	
IS200/IS605 family transposase IS200C	X	
IS5 family transposase IS903	X	
Nitrate/nitrite sensor protein NarX	X	
Hypothetical protein (3)	X	
IS3 family transposase ISEcl1		X
Hypothetical protein (2)		X

Bacteria-free FMT filtrate used to check for presence of phage in FMT doses was prepared by centrifuging a sample of an FMT dose at 3 g for 2 hours, then filtering the supernatant through a 0.2 µm filter. This filtrate was spot-tested on a lawn of each bank *E. coli* isolate and *E. coli* C. The density of phage in FMT doses was below the limit of detection for this test; less than 10^2 PFU/mL. While FMT phage titers are undetectable, FMTs can be enriched to increase phage titers in two methods. Incubating 250mL of FMT dose mixed with 500mL LB broth at 37 °C overnight yields a lysate of $>10^3$ phage which plaque on bank *E. coli*, while incubating FMT dose alone at 37 °C overnight yields lysate of ~10^2 phage that do not plaque on bank *E. coli*, only *E. coli* C (data not shown). Presence of phage was evaluated as described. To isolate clonal phage, for each of 5 FMT-sourced bacterial isolates, single plaques were picked using a sterile stick and serially streaked out on phage plates, with a lawn of that isolate poured on top. After a total of 3 serial streakings, single plaques were picked and lystate of these plaques was prepared. These 13 lysates comprised the bank of FMT-sourced phage isolates. Whole-genome sequencing and subsequent alignment of bank phage showed 4 homology regions among isolates (Fig. 2).

Assessment of phenotypic diversity of bank phages was performed through analysis of the relative efficiency of plating (EOP) of each phage through previously described methods (Kutter, 2009). Briefly, titers of each bank phage lysate were compared to the maximum titer observed. For these FMT-sourced phage, the maximum titer was always observed against *E. coli* C. Despite much sequence homology between bank *E. coli* and bank phage, differences in plating efficiency was observed (Fig. 3).

Figure 2. Aligned genomes of 13 FMT-sourced bank phage in descending order of length. Assembled genome contigs are mostly comprised of homologous regions. Green, blue, and cyan homologous regions are shared among all phage, while the red regions is shared among 11/12 phage.

	ϕB2-2	ϕA8L-1	ϕA5-3	ϕA8L-2	ϕA2-2	ϕA5-2	ϕA5-1	ϕB1-2	ϕA1-2	ϕB1-1	ϕA8L-3	ϕB2-1	ϕA2-1
D4L	0.09	0.08	0.08	0.11	0.12	0.12	0.13	0.13	0.22	0.15	0.14	0.21	0.50
B9	0.13	0.12	0.14	0.15	0.16	0.15	0.13	0.15	0.17	0.17	0.19	0.25	0.60
A9	0.13	0.12	0.14	0.17	0.14	0.12	0.12	0.16	0.18	0.26	0.23	0.28	0.60
A3	0.13	0.11	0.11	0.14	0.17	0.14	0.16	0.14	0.19	0.25	0.21	0.30	0.69
A1	0.13	0.14	0.16	0.14	0.16	0.19	0.19	0.20	0.21	0.19	0.18	0.32	0.61
B6	0.15	0.16	0.15	0.18	0.14	0.15	0.15	0.18	0.19	0.23	0.24	0.32	0.64
A4	0.16	0.19	0.19	0.21	0.20	0.24	0.22	0.21	0.30	0.24	0.30	0.38	0.81
C2L	0.21	0.22	0.22	0.19	0.21	0.28	0.30	0.26	0.28	0.28	0.31	0.42	0.87
E. coli C	1.00	1.00	1.00	1.00	1.00	1.00	1.00	1.00	1.00	1.00	1.00	1.00	1.00

More plaquing

Less plaquing

Figure 3. EOP of bank phage on bank *E. coli* plus *E. coli* C, average of 3 biological replicas. Plating efficiency of bank phage on *E. coli* C was averaged between 3 biological replicas and served as a normalization factor for plating efficiency of each bank phage. Bank phages display a wider range of EOP across bank isolates than expected natural biological variation, as do bacteria across multiple phages. Genetic Clades colored according to Clade (1: green, 2: gold).

The expected biological variance in plaquing for a either a single bank phage across multiple *E. coli* or multiple bank phage with a single bank *E. coli* was established to be 37% of the EOP (Table S2). To assess the significance of these variances, Dunn's test was conducted for all bank *E. coli* and bank phage (Fig. 4, Fig. 5). Broadly, bank phage display significantly wide ranges of EOP across bank *E. coli* despite similarity in genomic structure. Most remarkably, pairs ϕA2-1/ϕB2-2 and ϕA8L-3/ϕA2-2 both share identical homologous region patterns, yet both display significant differences in plating efficiency across isolates. This trend is also apparent within the bacterial isolates. As discussed previously, the small number of nucleotide sequence variants in bank *E. coli* genomes would classify them as a single *E. coli* strain by most criteria, and perhaps even a single Clade within that strain. Yet, *E. coli* D4L separates from the rest of its Clade, having much lower EOP than the other 3 isolates with an associated p-value <0.05. At the same time, Clade two is evenly split between the top and bottom of the EOP matrix, and members are display distinctly different phage susceptibilities in 4/6 combinations of member. Differences genomic structure also do not correspond to difference in plating efficiency for phage. This can be seen from pairs such as ϕA2-2 and ϕA5-2, which share the most difference in genomic structure observed in bank phages. However, their difference in plaquing efficiency have no statistical significance (associated p-value is >0.05).

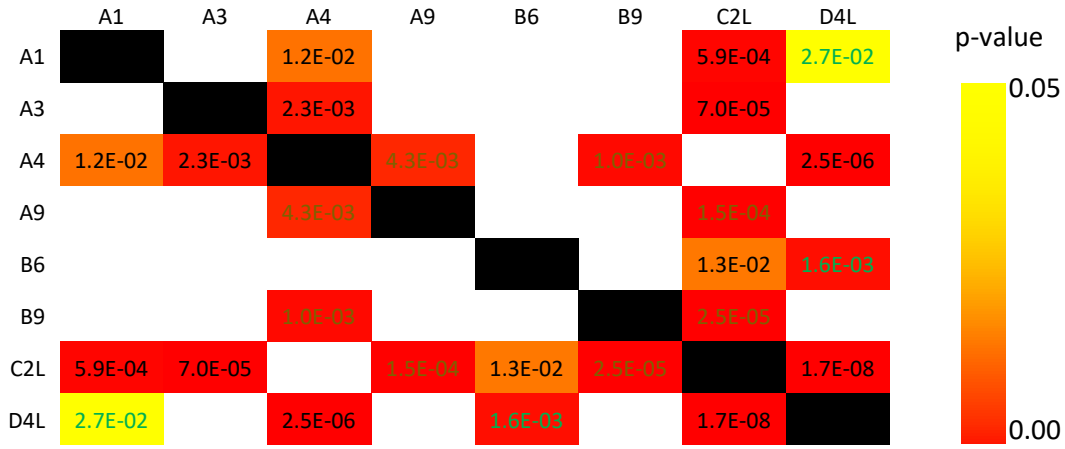

Figure 4. Dunn's test p-values <0.05 for bank *E. coli* isolates. Value indicate that host is a statistically significant factor of plating efficiency for colored values. Blank spaces fail to reject null hypothesis, and have no statistical significance of differences. Pairs colored according to within-Clade isolates (1: green, 2: gold).

The observed EOP differences of FMT-sourced *E. coli* and FMT-sourced phage show phenotypic differences in isolates which share great sequence homology. Understanding the cause of these differences among *E. coli* isolates has been difficult to elucidate, and much further work is required. Restriction-modification systems (RMSs) are theoretically capable of providing the differences in EOP, and RMSs are frequently on plasmids, who's sequence identity would be missed by genome assembly. If a bacteria possesses a RMS, then co-incubated phage would have its genetic material modified and thus be attenuated to that bacteria. A preliminary test (one replica) using the two most extremely phenotypically different *E. coli* and phage isolates, D4L with ϕB2-2 and C2L with ϕA2-1 was conducted. Approximately 10^6 bacteria and 10^8 phage were combined in liquid LB and cultured at 37 °C for 24 hours. Cultures were then passed through a 0.2 µm filter and lysates were spotted on bank *E. coli* isolates. EOP of attenuated phage is reduced across all *E. coli* isolates, which would not have observed if

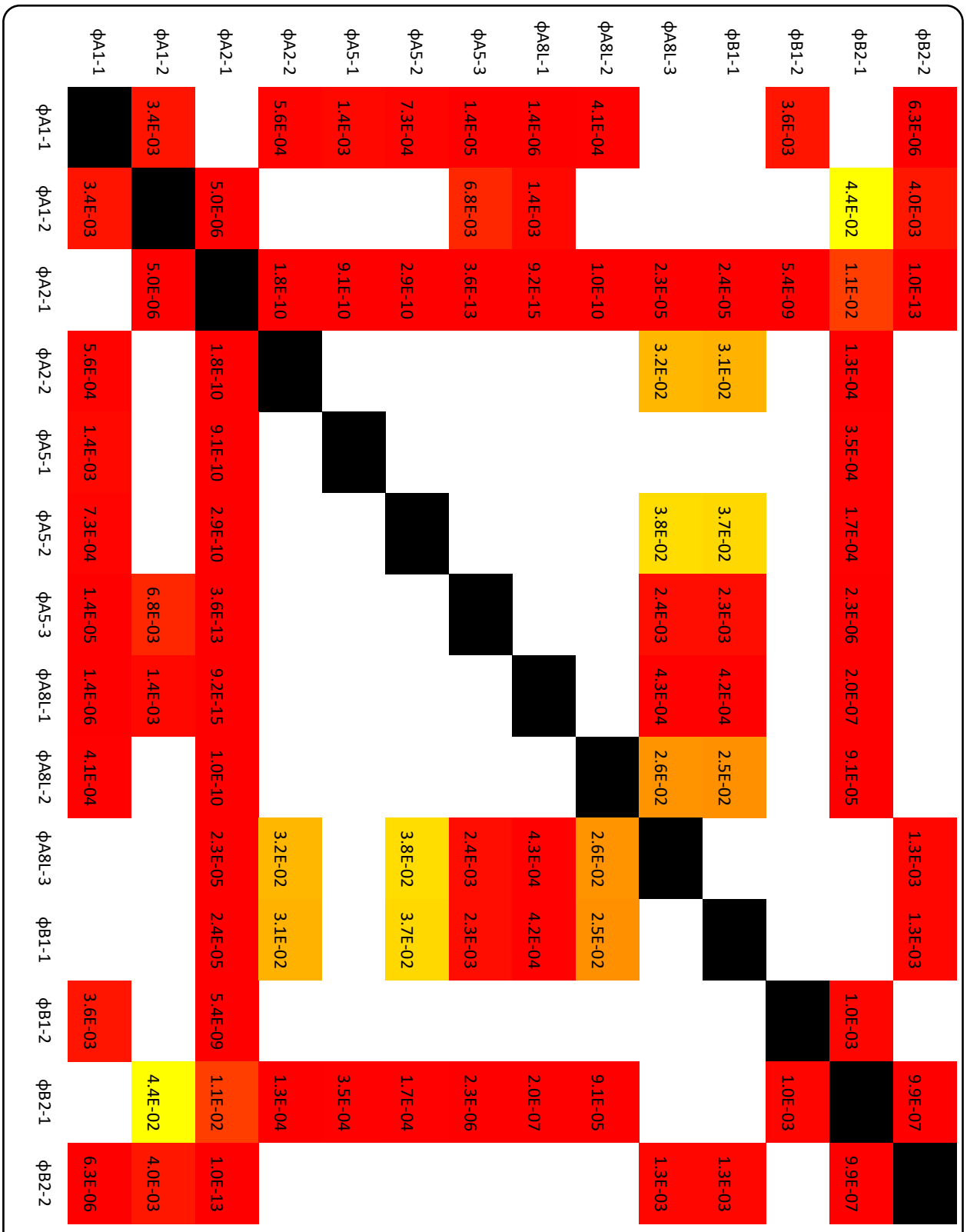

Figure 5. Dunn's test p-values <0.05 for bank phage isolates. Value indicate that host is a statistically significant factor of plating efficiency for colored values. Blank spaces fail to reject null hypothesis, and have no statistical significance of differences.

bank *E. coli* possessed different RMSs (Table 2). However, susceptibility to phage changed across isolates. Bank isolates with a higher or lower EOP than others in Figure 3 did not always display this degree of susceptibility in the test against attenuated phages. This phenomenon warrants further investigation.

Table 2. Isolate-attenuated phage infectivity against other isolates. 1 replica.

Isolate	EOP on ΦA1-2 grown on C2L	EOP on ΦB2-2 grown on D4L
A1	0.020	0.015
A3	0.033	0.026
A4	0.013	0.012
A9	0.010	0.011
B6	0.027	0.026
B9	0.019	0.019
C2L	0.013	0.012
D4L	0.020	0.016
C	1.000	1.000

Another factor common of resistant populations of bacteria is evolutionary cost. If phage-resistant strains grow more poorly than cohabiting susceptible strains, then susceptible bacteria may be able to outcompete them, even in the presence of phage. 4 *E. coli* isolates were selected to develop resistance to each of 4 selected phages. Tracking the optical density at 600nm (OD_{600}) serves as a proxy by which to measure the growth patterns of *E. coli* isolates is liquid LB media. However, resistant isolates do not have significantly slower growth rates or lower stationary phase densities than the susceptible strains (Fig. 6).

Discussion

E. coli and their phages were isolated from FMT doses. It was found that culturable phage densities of FMT doses are extremely low, yet can easily be enriched. Enrichment by simple incubation of FMT doses interestingly yields a moderately low (10^2) titer of phage that can only form plaques on *E. coli* C. This strain lacks any restriction-modification systems, and relies entirely on randomly-evolved envelope resistance to guard against phage. However, the addition of nutrient media creates a higher titer of phage (>10^3), which can also form plaque on wild, FMT-sourced *E. coli* isolates. Phages appear to be maintained at low-levels in FMTs, and this is consistent with experiments in nutrient media (Fig. S1). However, in experiments in nutrient media, resistance quickly evolves, yet FMT-sourced phage are capable of infecting and replicating on all isolates of *E. coli* sourced from FMTs of same individual. If phage-sensitive cells are abundant (>10^6/mL), then it would be expected that density of these lytic phages would ascend and phages would be greatly abundant in FMT doses. This would also provide selective pressure towards resistance. However, none of these *E. coli* isolates showed full resistance to the phages. In addition, liquid cultures of *E. coli* isolates can readily evolve resistance against these phages in a matter of hours (data not shown). A possible explanation that requires investigation is that, at least in the case of *E. coli*, the bacteria are not highly metabolically active. Slow-growing bacteria may

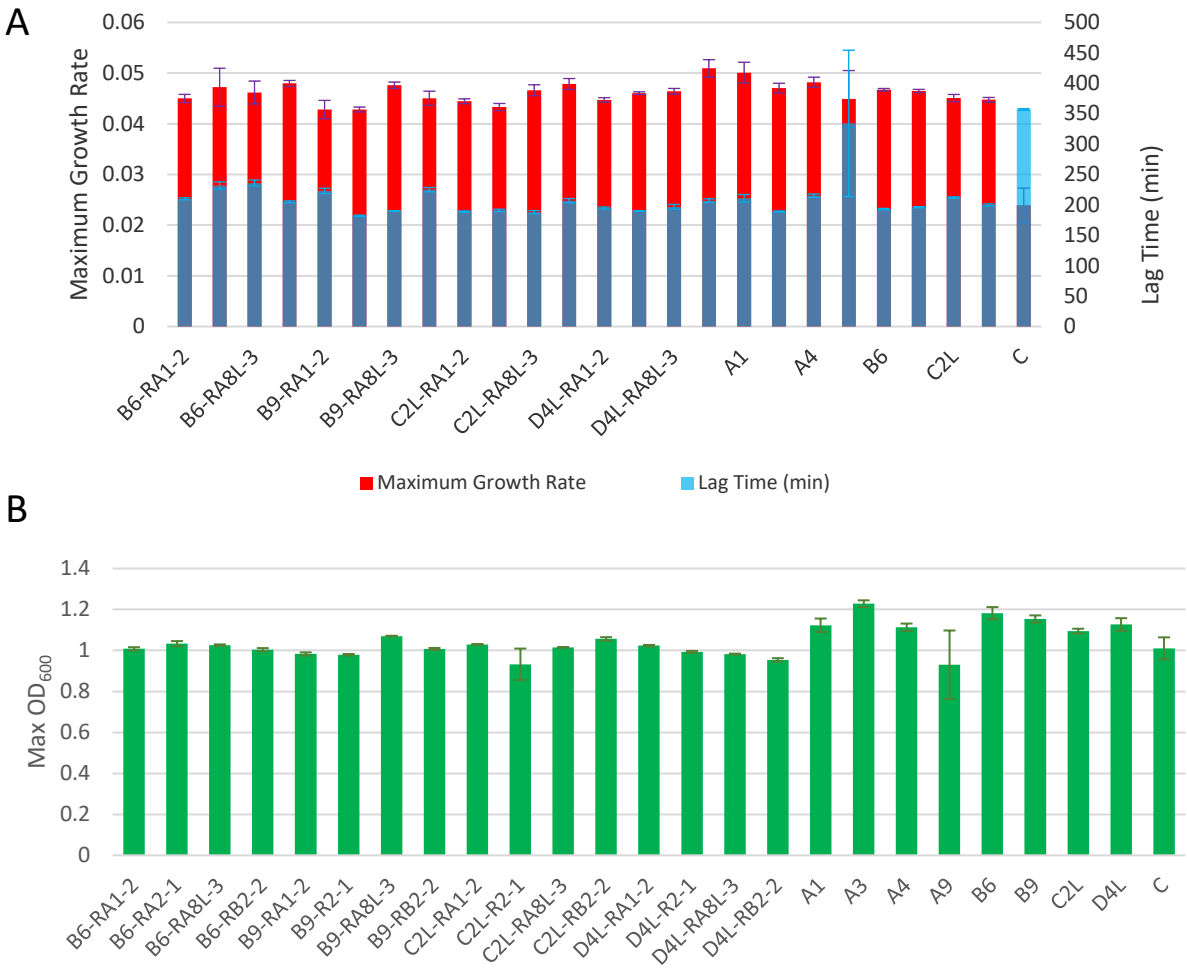

Figure 6. Growth data for phage-resistant *E. coli* isolates, average values of 5 replicates with standard error. **A.** Maximum growth rate and lag time for each resistant isolate as well as bank *E. coli* isolates. Growth rate in arbitrary units. **B.** Maximum OD_{600} used a proxy for maximum bacterial cell density in liquid culture of LB media.

not be able to support dense phage population regardless of sensitivity. One consideration is that in anaerobic conditions, *E. coli* show reduced growth rate and differentially express many genes (von Wulffen, et. al., 2016). The lack of bioavailable nutrients in the gut may also contribute to a slower growth rate of *E. coli* compared to that in LB, a rich media. Analyses of growth dynamics in FMTs and raw stool should be pursued. In addition, the gut should not be considered as an isolated culture of bacteria and phage; there is a regular effluent of these populations from the gut, which may have a significant effect on the population dynamics of bacteria and phage, especially if those bacteria are growing relatively slowly. Models of the population dynamics in these conditions can be found in appendix 1.

Genetic variation among *E. coli* isolates was very low, with only 37 variable genes found among 8 isolates from a single FMT donor. High sequence identity, with a detection of 32 ± 17 SNPs among common genes indicates that all isolates may have originated from a single clade. Single strains of *E. coli* form Clades with a variance of 17-30 SNPs (Li et. a., 2021; Ludden et. a., 2021). Further work is needed

to evaluate the functional impacts that might be expected based on the annotation of the genes in which these SNPs were detected.

Despite their high genetic similarity, *E. coli* D4L phenotypic susceptibility to phage does not cluster with other Clade 1 members in the EOP matrix; bank phages are less able to (or are much slower to) infect and replicate on D4L. Nucleotide sequence analyses did not correlate with phenotypic infectivity for bank phages as well. The most genetically similar bank phages are on opposite ends of the EOP matrix. ϕA2-1 forms plaques on most isolates nearly twice as well as any other phage, and in the cases of A4 and C2L, is nearly as infectious on those *E. coli* as *E. coli* C. This strain provided the highest plating efficiency on account of its lack of defense systems, allowing phage to infect and replicate uninhibited. This observation generates a potential mechanism which accounts for the variation among bacteria.

We have shown here that the genomic approaches appear insufficient to predict susceptibility and wild *E. coli* and their phage. These findings suggest that substantial phenotypic susceptibility can be observed despite high genetic similarity. This has important implications for the rational design of phage therapeutics and in the development of phage susceptibility clinical diagnostics. An Individual bacterial or phage isolate may show different plating efficiency on strains with incredibly low genetic variation. These trends show that culture-based methods are essential for the study of the ecological interactions between bacteria and phage in the gut microbiome.

Materials and Methods

Strains and Growth Media. Lysogeny broth (LB) prepared according to manufacturer instructions (Difco, REF 244620). LB soft agar made with 0.7% w/v agarose, and LB plates made with 1.6% agarose, LB phage plates prepared as LB plates supplemented with 20 mM $CaCl_2$. Supplemented brain-heart infusion (BHIS) media prepared as described (SOURCE): 37% w/v BHI Broth powder (HIMEDIA, REF M210I), 2% w/v sodium bicarbonate, 1% w/v L-cysteine, 0.005% w/v hemin (Sigma-Aldrich, REF H9039), with BHIS soft agar made with 0.7% w/v agarose, BHIS plates made with an additional 1.6% agarose, and BHIS phage plates made as BHIS plates supplemented with 20mM $CaCl_2$.

Lysates of FMT-derived phage were prepared from single plaques at 37 °C in LB broth alongside specified *E. coli* isolate by plate lysis. Specifically, individual plaques were picked with a sterile stick, resuspended in 4 mL of soft agar with 0.1 mL of overnight bacterial culture and plated on top of phage plates (lawn). The plates were then incubated at 37 °C overnight and this phage isolation protocol repeated. Then, single plaques were picked with a sterile stick and swirled in LB media and a colony of the specified *E. Coli* isolate was added, and these cultures were incubated at 37 °C for 5 hours. The lysates were then centrifuged at 3 g for 2 hours, sterilized via syringe-driven filtration through 0.2 µm filter (basix, REF 13-1001-06), and stored at 4 °C.

Sampling Bacterial and Phage Densities. Bacteria and phage densities were estimated by serial dilutions in 0.85% NaCl solution followed by plating. The total density of bacteria was estimated on LB plates. To

estimate the densities of phage, cultures were centrifuged at 3 g for 10 minutes and passed through a 0.2µm filter before serial dilution. These suspensions were mixed with 0.1 mL of overnight LB grown cultures of specified bacteria in 4 mL of LB soft agar and poured onto phage plates.

E. coli Isolation from FMTs. Serial dilutions of FMT in 0.85% NaCl solution was followed by plating on LB plates. Individual colonies were randomly chosen and picked with a sterile stick and simultaneously streaked onto an EMB plate (HIMEDIA, REF MM022) and a DM plate (Sigma-Aldrich, REF 15758), supplemented with 0.4% w/v lactose (Sigma-Aldrich, L3750). Both were incubated at 37 °C overnight. Isolates colored green on the EMB plate were serially streaked from the DM lactose plate onto another DM lactose plate and incubated at 37 °C overnight. Isolates were again serially streaked onto an DM lactose plate and incubated at 37 °C overnight. Single colonies were put up in LB media and incubated at 37 °C overnight. 0.5mL of this culture was combined with LB with 15% glycerol and stored at -80°C.

Sequencing. Isolate 16S genes were amplified via hot-start PCR. PCR product was run on a 1% agarose gel electrophoresis with 1X GelRed (Biotium, REF 41003). Bands were visualized on a Fotodyne Foto/Prepl UV-Transilluminator 3-3500 and excised. DNA was purified by using a PureLink™ Quick Gel Extraction Kit. Purified 16S DNA was sequenced via Sanger sequencing (using the primers forward: 5'-CGG TTA CCT TGT TAC GAC TT-3' and reverse: 5'-AGA GTT TGA TCC TGG CTC AG-3') by Eurofins Scientific (Kentucky, USA). Resulting sequences were analyzed using NCBI BLAST (January, 2022).

Individual clones of *E. coli* isolate genomic DNA was prepared by using a Zymo Research Quick-DNA HMW MagBead Kit (REF D6060) according to manufacturer instructions. Illumina pair-ended libraries were prepared from genomic DNA and sequenced by the Microbial Genome Sequencing Center Pittsburg (MiGS). The gaps in these assemblies were completed using Oxford Nanopore 300Mbp Long Reads also performed by MiGS. Phage DNA was extracted from cell-free lysate by using an Invitrogen PureLink™ Viral RNA/DNA Mini Kit (REF 12280-050) according to manufacturer instructions. Isolate DNA was sequenced using an Oxford Nanopore according to manufacturer instructions. Reads were assembled using the Flye assembler and aligned using Mauve, both in Geneious Prime® 2022.1.1, Build 2022-03-15 11:43, Java Version 11.0.14.1+1 (64 bit). Resulting sequences were analyzed using NCBI BLAST (March, 2022).

Plasmid restriction digest. Isolate plasmids of *E. coli* isolates were extracted and purified using a GenElute HP Plasmid Miniprep Kit (Sigma, REFNA0160-1KT). Approximately 100ng of plasmid was combined with 5uL buffer, 34uL molecular-grade water (HIMEDIA, REF TCL018), and 1uL BamHI-HF, EcoRi-HF, HindIII-HF, or NdeI (New England Biolabs, REF R3136S, R3101S, R3104S, and R0111S, respectively). Solutions were incubated for 20 minutes at 37 °C, then reactions using EcoRI-HF or NdeI were terminated by incubating solutions at 60 °C for 20 minutes, and reactions using HindIII-HF were terminated by incubating solutions at 80 °C for 20 minutes. Product was run on a 1% agarose gel electrophoresis with 1X GelRed (Biotium, REF 41003) and visualized with a

Antimicrobial Susceptibility. *E. coli* isolates were sent to the Emory University Hospital Microbiology Lab for assessment of their antimicrobial susceptibility profiles utilizing a VITEK system.

Statistical Analysis. Dunn's test was conducted in R 4.1.3 (2022-03-10) – "One Push-Up" (Copyright 2022 The R Foundation for Statistical Computing) using the Simple Fisheries Stock Assessment Methods (FSA) package by Derek Ogle.

Supplementary Data

Table S1. Source and Identity of FMT-sourced bacterial isolates for assessment of frequency of *E. coli* among fast-growing aerobes isolated from FMT doses. Isolates in bold species' identity is acquired from whole-genome sequencing rather than 16S sequence.

Isolate	Donor ID	Species	Top 16S BLAST hit Genbank ID
A1	**MEPSD-06**	***E. coli***	**CP079884.1**
A2	MEPSD-06	*E. coli*	CP076232.1
A3	**MEPSD-06**	***E. coli***	**AY319393.1**
A4	**MEPSD-06**	***E. coli***	**CP079884.1**
A5	MEPSD-06	*E. fergusonii*	CP079884.1
A6	MEPSD-06	*E. fergusonii*	CP079884.1
A7	MEPSD-06	*E. coli*	CP076232.1
A8L	MEPSD-06	*E. coli*	KJ803899.1
A8S	MEPSD-06	Staphylococcus sp.	HM051082.1
A9	**MEPSD-06**	***E. coli***	**CP079884.1**
A10	MEPSD-06	*E. fergusonii*	CP079884.1
B1	MEPSD-06	Enterobacteriaceae sp.	KX688070.1
B2	MEPSD-06	*Bacillus cereus*	KR822284.1
B3	MEPSD-06	*Shigella flexneri*	CP054892.1
B4	MEPSD-06	*Shigella boydii*	KY776568.1
B5	MEPSD-06	*E. coli*	CP076232.1
B6	**MEPSD-06**	***E. coli***	**CP079884.1**
B7	MEPSD-06	*E. coli*	CP076232.1
B8	MEPSD-06	*E. fergusonii*	CP079884.1
B9	**MEPSD-06**	***E. coli***	**CP041538.1**
B10	MEPSD-06	*E. fergusonii*	CP079884.1
G1	**SD-01**	***E. coli***	**CP076232.1**
G2	SD-01	*E. coli*	CP076232.1
G3	**SD-01**	***E. coli***	**CP053597.1**
G4	SD-01	*E. coli*	CP076232.1
G5	SD-01	*E. coli*	AP022362.1
G6	SD-01	*E. coli*	CP076232.1
G7	SD-01	*E. coli*	CP076232.1
G8	SD-01	*E. coli*	CP076232.1
G9	SD-01	*E. coli*	CP076232.1
G10	SD-01	*E. coli*	CP076232.1

Table S2. Multiple biological replicas of EOP. Total plaque counts given for each replica, including original 3 replicas of EOP assay.

Replica	1	2	3	4	5	6	7	8	9	10	EOP 1	EOP 2	EOP 3
A1 & A2-1	530	390	320	320	290	260	240	180	300	440	210	180	240
A1 & A8L1	500	380	310	350	300	250	330	430	210	340	410	260	103
A3 & A2-1	560	270	280	310	290	370	460	440			210	200	180
A3 & A8L-1	50	390	280	280	170	220	430	380	350	420	440	170	250
D4L & A2-1	490	320	400	370	340	250	320	220	230	310	145	210	70
D4L & A8L-1	470	380	300	350	305	260	260	460	280	370	180	150	100

Table S3. Efficiency of plating for bank phage on *E. coli* C, performed in biological triplicate

Replica	ϕA1-1	ϕA1-2	ϕA2-1	ϕA2-2	ϕA5-1	ϕA5-2	ϕA5-3	ϕA8L-1	ϕA8L-2	ϕA8L-3	ϕB1-1	ϕB1-2	ϕB2-1	ϕB2-2
1	50	41	27	75	60	87	90	98	78	110	60	106	58	74
2	63	75	14	103	56	85	73	85	74	87	73	92	46	76
3	59	66	10	105	60	63	83	67	58	92	83	86	27	70

Table S4. Efficiency of plating for bank phage on bank *E. coli* isolates, performed in biological triplicate

	ϕA1-1	ϕA1-2	ϕA2-1	ϕA2-2	ϕA5-1	ϕA5-2	ϕA5-3	ϕA8L-1	ϕA8L-2	ϕA8L-3	ϕB1-1	ϕB1-2	ϕB2-1	ϕB2-2
A1	0.309	0.223	0.776	0.286	0.317	0.356	0.311	0.295	0.223	0.277	0.142	0.326	0.536	0.221
A3	0.277	0.168	0.741	0.178	0.138	0.107	0.095	0.104	0.154	0.212	0.271	0.127	0.227	0.086
A4	0.502	0.445	1.076	0.245	0.286	0.318	0.285	0.317	0.283	0.439	0.167	0.311	0.433	0.217
A9	0.262	0.129	0.776	0.204	0.128	0.157	0.135	0.13	0.189	0.262	0.3	0.168	0.302	0.147
B6	0.314	0.163	0.882	0.13	0.143	0.184	0.11	0.13	0.189	0.212	0.275	0.168	0.35	0.131
B9	0.23	0.188	0.812	0.184	0.143	0.176	0.139	0.158	0.18	0.206	0.208	0.139	0.289	0.155
C2L	0.413	0.336	0.953	0.273	0.322	0.337	0.274	0.223	0.21	0.405	0.183	0.323	0.433	0.209
D4L	0.795	0.203	0.512	0.099	0.077	0.08	0.059	0.065	0.069	0.131	0.042	0.086	0.103	0.033
A1	0.272	0.218	0.635	0.127	0.133	0.161	0.117	0.094	0.129	0.174	0.267	0.184	0.302	0.098
A3	0.293	0.138	0.706	0.159	0.164	0.191	0.154	0.122	0.163	0.274	0.267	0.152	0.371	0.139
A4	0.314	0.168	0.776	0.204	0.184	0.214	0.146	0.122	0.206	0.262	0.333	0.171	0.426	0.139
A9	0.241	0.257	0.671	0.191	0.184	0.138	0.249	0.173	0.249	0.28	0.325	0.209	0.33	0.155
B6	0.126	0.143	0.512	0.13	0.118	0.165	0.209	0.22	0.206	0.339	0.167	0.2	0.405	0.143
B9	0.136	0.148	0.565	0.146	0.066	0.115	0.154	0.115	0.111	0.193	0.167	0.139	0.151	0.076
C2L	0.502	0.405	1.235	0.242	0.409	0.383	0.307	0.324	0.24	0.311	0.45	0.292	0.591	0.286
D4L	0.335	0.287	0.741	0.153	0.225	0.176	0.139	0.108	0.18	0.174	0.25	0.203	0.357	0.147
A1	0.157	0.178	0.424	0.064	0.113	0.054	0.04	0.037	0.056	0.093	0.167	0.095	0.124	0.074
A3	0.324	0.277	0.635	0.184	0.184	0.126	0.095	0.09	0.103	0.143	0.225	0.152	0.289	0.164
A4	0.22	0.287	0.565	0.159	0.194	0.176	0.146	0.122	0.154	0.193	0.225	0.158	0.289	0.123
A9	0.178	0.148	0.353	0.035	0.061	0.061	0.048	0.043	0.073	0.149	0.158	0.114	0.22	0.09
B6	0.241	0.257	0.529	0.153	0.194	0.107	0.132	0.13	0.137	0.181	0.233	0.165	0.206	0.164
B9	0.241	0.168	0.424	0.14	0.194	0.169	0.139	0.101	0.146	0.174	0.133	0.158	0.302	0.164
C2L	0.167	0.101	0.424	0.121	0.164	0.123	0.08	0.101	0.111	0.206	0.217	0.171	0.247	0.139
D4L	0.188	0.168	0.247	0.108	0.092	0.092	0.051	0.072	0.086	0.118	0.15	0.095	0.165	0.082

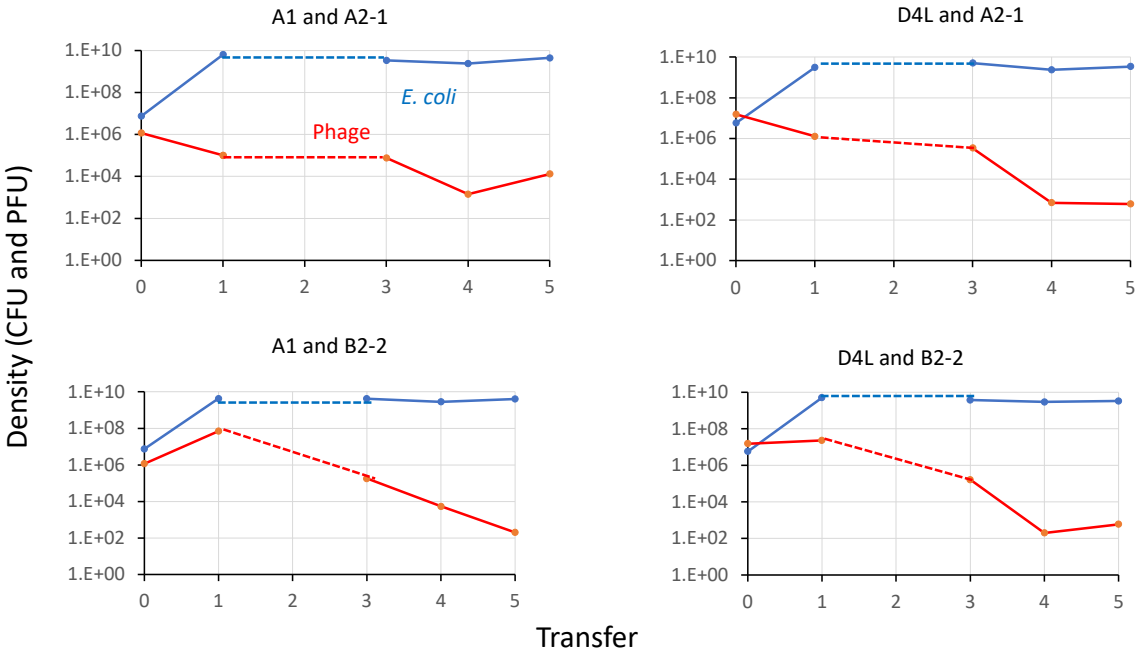

Figure S1. Serial transfer experiment of *E. coli* isolate and phage. 1/100 dilutions of culture were prepared each day for 5 days, and the density of bacteria and phage were each checked. Resistant mutants ascend within 24 hours, and phage are slowly lost, but maintained, within 5 days.

Appendix 1

Isolating phage from FMTs by adding resources

The results of experiments indicate that by adding resources (nutrients) to the FMTs, high densities of phage can be recovered. We postulate that this occurs because there is a dearth of resources in the FMTs which limit the ability of the bacteria and phage to replicate. When resources are added, the density of phage sensitive bacteria increases, and the phage replicate. The density of bacteria and phage in these enriched FMT cultures, levels off when the added resources are consumed. This process can be seen from a simple model of the population dynamics of bacteria and phage.

In this model there are two populations of bacteria, sensitive and resistant (refractory) to the phage and a single population of phage, with densities (cells or particles per ml) and designations, N and NR and P, respectively. The bacteria adsorb to the phage with a rate constant, □ ml per cell per hour, and infections produce, □, phage per infected cell, the burst size. The sensitive cells have a maximum growth rate of V cells per hour for the phage sensitive bacteria, and V*(1-a) for the resistant. If a is positive, the resistant cells have a growth rate disadvantage.. The density of the bacterial population is limited by a resource, R µg/ml/. The realize growth rate is the product of the maximum growth rate hyperbolic function of the concentration of the resource {Monod, 1949 #43}, $\gamma(r) = \frac{R}{(R+k)}$. The parameter *k*, the Monod constant, is the concentration of the resource where the growth rate is half it's maximum value. To produce a new cell, e µg/ml of the resource is consumed {Stewart, 1973 #44}. To account for the decline in the rate of successful phage infection with declines in the resource concentration, we the realized phage adsorption rate parameter is proportional to the concentration of the resource, □*□(R). With these definitions and assumptions, the rates of change in the densities of bacteria and phage and the concentration of the resource are given by the following set of coupled differential equations.

$$\frac{dR}{dt} = -\gamma(r)\cdot e\cdot(v\cdot N - v\cdot(1-a)\cdot NR$$

$$\frac{dN}{dt} = v\cdot N\cdot\gamma(r) - \delta\cdot\gamma(r)\cdot N\cdot P$$

$$\frac{dNR}{dt} = v\cdot(1-a)\cdot N\cdot\gamma(r)$$

$$\frac{dP}{dt} = \delta\cdot\gamma(r)\cdot N\cdot P\cdot(b-1)$$

By letting the burst be (□-1), we are accounting for the loss of the infecting phage.

In Figure 1 we follow the changes in the densities of bacteria and phage, and the concentration of a limiting resource in a batch culture. In a habitat with dearth of the limiting resource Figure 1 (A), the bacteria grow to a density of ~ $2x10^5$ and the phage density increases slightly, from 10 PFU to 16 PFU. In runs that follow, we initiate the simulated population with $N=2x10^5$ and P=16 . When 1000µg/ml of resource is added to the habitat with a dearth of resource, the phage density rapidly increases, Figure 1(B). If resource is added and the adsorption rate consistent is lower, $\delta=10^{-8}$ rather than 10^{-7}, the ascent

of the phage is somewhat reduced, but the density of phage produced is greater (Figure 1(C)). If phage resistant bacteria are present, following enrichment with the resource the phage density increases, as does the resistant bacterial population.

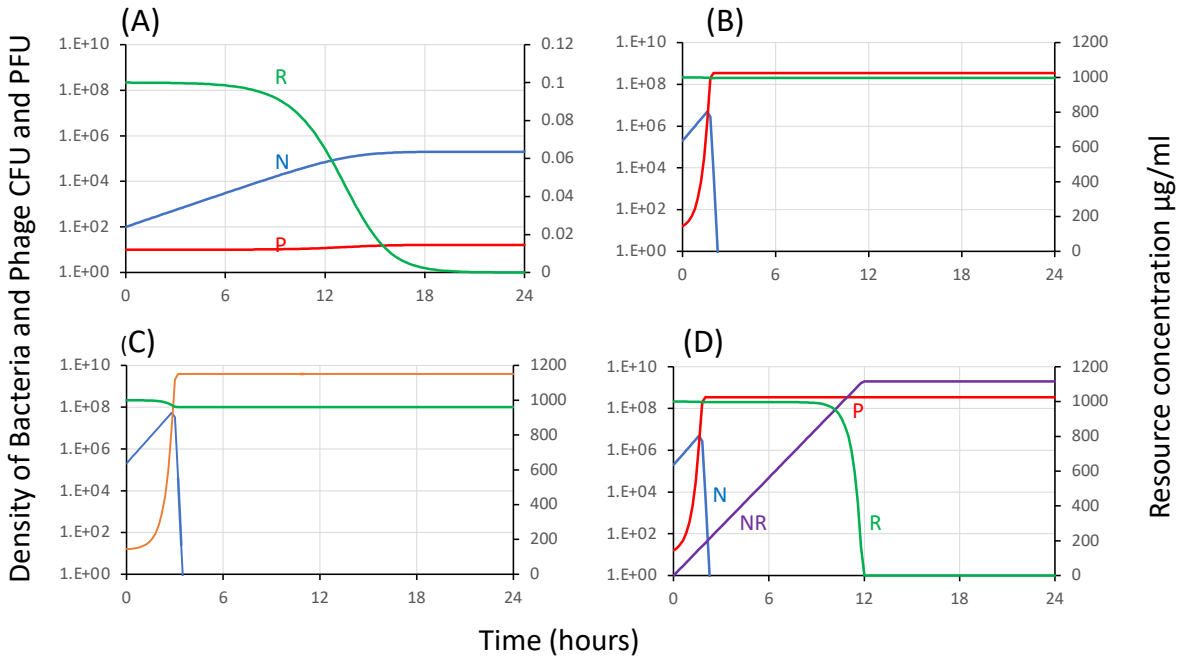

Figure A1. Simulation, changes in the densities of sensitive, N, (blue) and resistant, NR, (purple) bacteria, phage, P, (red) and the concentration of a limiting resource, R. (green). Standard parameters, v=2.0 per hour, a=0.1, k=0.25 µg/ml, e=5x10^{-7}, □=10^{-7}, □=50. (A) bacteria and phage becoming established environment with a dearth of resource, R_{MAX}=0.1 µg/ml. (B) 1000µg/ml of the limiting resource added to a population with the dearth of resource, the population in (A) at 24 hours. (C) Same as (B), but δ=10^{-8}. Same as (B) but initiated with a single resistant bacterium, NR.

References:

1. Amabebe, E., Robert, F. O., Agbalalah, T. & Orubu, E. S. F. Microbial dysbiosis-induced obesity: role of gut microbiota in homoeostasis of energy metabolism. *British Journal of Nutrition* **123**, 1127–1137 (2020).
2. Cammarota, G. *et al.* Randomised clinical trial: faecal microbiota transplantation by colonoscopy vs. vancomycin for the treatment of recurrent *Clostridium difficile* infection. *Alimentary Pharmacology & Therapeutics* **41**, 835–843 (2015).
3. Canakis, A., Haroon, M. & Weber, H. C. Irritable bowel syndrome and gut microbiota. *Curr Opin Endocrinol Diabetes Obes* **27**, 28–35 (2020).
4. Chandrasekaran, R. & Lacy, D. B. The role of toxins in *Clostridium difficile* infection. *FEMS Microbiol Rev* **41**, 723–750 (2017).
5. Chidambaram, S. B. *et al.* Gut dysbiosis, defective autophagy and altered immune responses in neurodegenerative diseases: Tales of a vicious cycle. *Pharmacol Ther* **231**, 107988 (2022).
6. Doh, Y. S. *et al.* Long-Term Clinical Outcome of *Clostridium difficile* Infection in Hospitalized Patients: A Single Center Study. *Intest Res* **12**, 299–305 (2014).
7. Fujimoto, K. *et al.* Functional Restoration of Bacteriomes and Viromes by Fecal Microbiota Transplantation. *Gastroenterology* **160**, 2089-2102.e12 (2021).
8. Gough, E., Shaikh, H. & Manges, A. R. Systematic Review of Intestinal Microbiota Transplantation (Fecal Bacteriotherapy) for Recurrent *Clostridium difficile* Infection. *Clinical Infectious Diseases* **53**, 994–1002 (2011).
9. Hota, S. S. *et al.* Oral Vancomycin Followed by Fecal Transplantation Versus Tapering Oral Vancomycin Treatment for Recurrent *Clostridium difficile* Infection: An Open-Label, Randomized Controlled Trial. *Clinical Infectious Diseases* **64**, 265–271 (2017).
10. Khoruts, A. & Sadowsky, M. J. Understanding the mechanisms of faecal microbiota transplantation. *Nat Rev Gastroenterol Hepatol* **13**, 508–516 (2016).
11. Kutter, E. Phage host range and efficiency of plating. *Methods Mol Biol* **501**, 141–149 (2009).
12. Lai, C. Y. *et al.* Systematic review with meta-analysis: review of donor features, procedures and outcomes in 168 clinical studies of faecal microbiota transplantation. *Aliment Pharmacol Ther* **49**, 354–363 (2019).
13. Leffler, D. A. & Lamont, J. T. *Clostridium difficile* Infection. *N Engl J Med* **372**, 1539–1548 (2015).

14. Lessa, F. C. *et al.* Burden of *Clostridium difficile* infection in the United States. *N Engl J Med* **372**, 825–834 (2015).

15. Li, D. *et al.* Genomic comparisons of Escherichia coli ST131 from Australia. *Microb Genom* **7**, 000721 (2021).

16. Ludden, C. *et al.* Defining nosocomial transmission of Escherichia coli and antimicrobial resistance genes: a genomic surveillance study. *The Lancet Microbe* **2**, e472–e480 (2021).

17. Madoff, S. E., Urquiaga, M., Alonso, C. D. & Kelly, C. P. Prevention of recurrent *Clostridioides difficile* infection: A systematic review of randomized controlled trials. *Anaerobe* **61**, 102098 (2020).

18. McDonnell, L. *et al.* Association between antibiotics and gut microbiome dysbiosis in children: systematic review and meta-analysis. *Gut Microbes* **13**, 1870402.

19. Mirzaei, M. K. & Maurice, C. F. Ménage à trois in the human gut: interactions between host, bacteria and phages. *Nat Rev Microbiol* **15**, 397–408 (2017).

20. Ni, J., Wu, G. D., Albenberg, L. & Tomov, V. T. Gut microbiota and IBD: causation or correlation? *Nat Rev Gastroenterol Hepatol* **14**, 573–584 (2017).

21. Ooijevaar, R. E. *et al.* Update of treatment algorithms for *Clostridium difficile* infection. *Clin Microbiol Infect* **24**, 452–462 (2018).

22. Ott, S. J. *et al.* Efficacy of Sterile Fecal Filtrate Transfer for Treating Patients With *Clostridium difficile* Infection. *Gastroenterology* **152**, 799-811.e7 (2017).

23. Pepin, J. *et al.* Increasing risk of relapse after treatment of *Clostridium difficile* colitis in Quebec, Canada. *Clin Infect Dis* **40**, 1591–1597 (2005).

24. Roy Sarkar, S. & Banerjee, S. Gut microbiota in neurodegenerative disorders. *J Neuroimmunol* **328**, 98–104 (2019).

25. Samore, M. H. Epidemiology of nosocomial *clostridium difficile* diarrhoea. *J Hosp Infect* **43 Suppl**, S183-190 (1999).

26. Schwartz, D. J., Langdon, A. E. & Dantas, G. Understanding the impact of antibiotic perturbation on the human microbiome. *Genome Med* **12**, 82 (2020).

27. Sheitoyan-Pesant, C. *et al.* Clinical and Healthcare Burden of Multiple Recurrences of *Clostridium difficile* Infection. *Clin Infect Dis* **62**, 574–580 (2016).

28. Smits, W. K., Lyras, D., Lacy, D. B., Wilcox, M. H. & Kuijper, E. J. *Clostridium difficile* infection. *Nat Rev Dis Primers* **2**, 16020 (2016).

29. Sokol, H. *et al.* Fecal microbiota transplantation to maintain remission in Crohn's disease: a pilot randomized controlled study. *Microbiome* **8**, 12 (2020).

30. Spigaglia, P., Mastrantonio, P. & Barbanti, F. Antibiotic Resistances of *Clostridium difficile*. in Updates on *Clostridium difficile* in Europe: Advances in Microbiology, Infectious Diseases and Public Health Volume 8 (eds. Mastrantonio, P. & Rupnik, M.) 137–159 (Springer International Publishing, 2018). doi:10.1007/978-3-319-72799-8_9.

31. Tauxe, W. M. *et al.* Fecal Microbiota Transplant Protocol for Clostridium Difficile Infection. *Lab Med* **46**, e19–e23 (2015).

32. Theriot, C. M. & Young, V. B. Interactions Between the Gastrointestinal Microbiome and *Clostridium difficile*. *Annu Rev Microbiol* **69**, 445–461 (2015).

33. van Nood, E. *et al.* Duodenal Infusion of Donor Feces for Recurrent *Clostridium difficile*. *New England Journal of Medicine* **368**, 407–415 (2013).

34. Wang, P. *et al.* Resveratrol-induced gut microbiota reduces obesity in high-fat diet-fed mice. *Int J Obes (Lond)* **44**, 213–225 (2020).

35. Weingarden, A. R. *et al.* Microbiota transplantation restores normal fecal bile acid composition in recurrent *Clostridium difficile* infection. *American Journal of Physiology-Gastrointestinal and Liver Physiology* **306**, G310–G319 (2014).

36. von Wulffen, J., Sawodny, O. & Feuer, R. Transition of an Anaerobic *Escherichia coli* Culture to Aerobiosis: Balancing mRNA and Protein Levels in a Demand-Directed Dynamic Flux Balance Analysis. *PLoS One* **11**, e0158711 (2016).

37. Zhang, Q., Cheng, L., Wang, J., Hao, M. & Che, H. Antibiotic-Induced Gut Microbiota Dysbiosis Damages the Intestinal Barrier, Increasing Food Allergy in Adult Mice. *Nutrients* **13**, 3315 (2021).